JOURNAL OF THEORETICAL AND APPLIED MECHANICS
50, 3, pp. 819-829, Warsaw 2012
50th Anniversary of JTAM

APPLICATION OF SPECTRAL METHOD IN FATIGUE LIFE ASSESSMENT – DETERMINATION OF CRACK INITIATION

Adam Niesłony, Michał Böhm
Opole University of Technology, Department of Mechanics and Machine Design, Opole, Poland
e-mail: a.nieslony@po.opole.pl; michalboehm@gmail.com

The purpose of this paper is to provide a simple approach for indication of those places of machine parts, where the fatigue crack initiation begins. This method uses FEM and the cyclic stress-strain curve for calculating the stress state on specimens. The multiaxial fatigue failure criterion based on the critical plane approach was used for reduction of the random spatial stress state into the equivalent uniaxial one. The critical plane position was established with the use of the variance method, and fatigue life was determined with assumption of linear damage accumulation. Experimental verification of the proposed method was performed with the use of results of fatigue tests for St52.3 structural steel subjected to biaxial random tension-compression. Cruciform specimens with four holes were tested. During the tests, the place and time of crack initiation were observed. It was shown, that the proposed method for determination of the places of fatigue crack initiation gave results well correlated with the data obtained from experiments. The proposed method could be applied by engineers in order to identify the places and time of fatigue cracks initiation.

Key words: spectral method, multiaxial fatigue, random loading, crack initiation

Notations

a_k	–	coefficients for multiaxial fatigue failure criteria, $k = (1, \ldots, 6)$
E	–	Young's modulus of elasticity [MPa]
F_{1-3}, F_{2-4}	–	forces applied to specimen arms 1-3 and 2-4, respectively, [kN]
f	–	frequency [Hz]
$\mathbf{L}(t)$	–	loading vector [kN]
t	–	time [s]
T_{cal}, T_{exp}	–	calculated and experimental obtained time to crack initiation, respectively, [s]
$\mathbf{G}_L(f), \mathbf{G}_\sigma(f)$	–	power spectral density matrix of loading vector $\mathbf{L}$ [kN^2/Hz] and of vector of strain tensor components [MPa^2/Hz], respectively
$\mathbf{Q}, \mathbf{Q}_H$	–	matrix of transition coefficients [kN^{-1}] and matrix of coefficients of generalized Hooke's law [MPa], respectively
m	–	coefficient of inclination of Wöhler's curve for tension-compression
l_η, m_η, n_η	–	directional cosines of vector normal to critical plane
M^+	–	expected rate of peaks
$N(\Delta\sigma)$	–	function which returns number of cycles for given stress range $\Delta\sigma$ from standard fatigue characteristic
N_0	–	number of cycle of knee point of Wöhler's curve
$p(\Delta\sigma)$	–	probability density function (PDF) of stress ranges
r_F	–	correlation coefficient according to forces $F_{1-3}(t)$ and $F_{2-4}(t)$
$\boldsymbol{\varepsilon}$	–	vector of strain tensor components

$\sigma_{eq}(t), \sigma_{af}$ – equivalent stress and fatigue strength, respectively, [MPa]
$\Delta\sigma_{tr}$ – stress range according to Neuber's rule [MPa]
ξ_k – k-th moment of PSDF
ν – Poisson's ratio
μ – variance [MPa^2]

1. Introduction

From considerations on damaged elements of machines or structures, it appears that material fatigue in the high-cycle range often appears in form of cracks (Manson, 1965; Stephens and Fuchs, 2001; Łagoda *et al.*, 2005; Niesłony and Macha, 2007; Schijve, 2009). Such failures are often observed in geometrically complex elements loaded by many independent random forces. In such cases, application of traditional methods of fatigue life determination, where the life is calculated in one point of the maximum fatigue intensity, is difficult because the position of that point is unknown. Evaluation of fatigue life of such elements is most often conducted by time-consuming and expensive experimental tests on the basis of which fatigue characteristics of entire elements or structure joints are designated. Received characteristics are highly individual, since they concern only one geometry and load type, and the problem of fatigue is treated globally. Therefore, an attempt to solve this problem by an experiment turned out to be insufficient and economically unjustified.

At the stage of machine element designing, static Finite Element Method (FEM) analyses are usually performed. As a result, maps of stresses or strains parameters, such as the stresses reduced according to the Huber-Mises hypothesis, are obtained. The values placed at geometry of the considered element as colored maps, allow evaluating the correctness of the designed element under static load. In many cases machine elements are dynamically loaded, so the designer has to take into account the future service conditions for the fatigue life assessment. Designers should assess when and where a fatigue crack could initiate. This complex task can be realised by applying known local methods of fatigue life determination and FEM (Niesłony and Sonsino, 2006; Niesłony, 2009). As a result of this type of analysis, we obtain a fatigue damage map similar to the well known stress map, which indicates the area of fatigue crack initiation for the current loading case. Furthermore, the obtainment of the expected fatigue life – the necessary parameter for further reliability analysis of the construction is at ease. In order to use the previous stages of design in an effective way, where we often perform static FEM calculations, the fatigue calculations use the models and results of the static FEM analysis performing the determination of crack initiation on the basis of postprocessing. In these types of analysis, the speed of calculations is also very important, because while preparing the fatigue life maps according to the local methods we need to compute the fatigue life several times, usually for every node of the finite element mesh. Therefore, the spectral method of fatigue life assessment is used, which is characterized as being more efficient than the cycle counting method (Pitoiset and Preumont, 2000; Łagoda *et al.*, 2005; Niesłony and Sonsino, 2006).

In this paper, the authors present an algorithm which allows one to determine the place of fatigue crack initiation with the use of FEM, and its verification based on fatigue tests of special cruciform specimens being subjected to tension-compression in two perpendicular directions.

2. Tests results used for verifying the fatigue crack initiation

The test results obtained for smooth or notched specimens subjected to combined bending with torsion (Macha and Niesłony, 2011) or tension-compression with torsion (Shamsaei *et al.*, 2011)

are usually applied for verification of algorithms of fatigue life assessment under multiaxial loading. Such tests allow one to load the specimen with any combination of the bending moment or the axial force and the torsional moment. Also, tests of cruciform specimens are performed in order to verify algorithms of multiaxial fatigue assessment (Zhang and Sakane, 2007). In the central part of the cruciform specimen, the plane stress state is obtained and suitable configuration of forces applied to the specimen arms, allow one to obtain variable or constant directions of principal stresses.

Determination of the fatigue crack initiation places in typical specimens used for fatigue tests seems to be trivial. The crack initiation occurs in one good known place where the maximum stress concentration can be observed. For smooth specimens, it is the cylindrical surface of the least diameter, for notched specimens – the neighborhood of the notch bottom (Niesłony, 2010), and for the cruciform specimens – their center (Łagoda *et al.*, 1999). Because of that, the test results presented in this paper concern special cruciform specimens where the place of fatigue crack initiation depends on loading configuration. Thus, in typical cruciform specimens presented in Fig. 1a four holes, 12 mm in diameter, were made. They were symmetrically arranged in relation to the arms along the radius of 26 mm, Fig. 1b. The specimens were made of St52.3 steel (sheets 8 mm in thickness), the specimen dimensions are presented in Fig. 1c. The chosen static and cyclic properties of the considered steel are shown in Table 1.

Table 1. Selected material properties of St52.3 structural steel

E [MPa]	ν	m	σ_{af} [MPa]	N_0
207000	0.28	7.9	205	$1.12 \cdot 10^6$

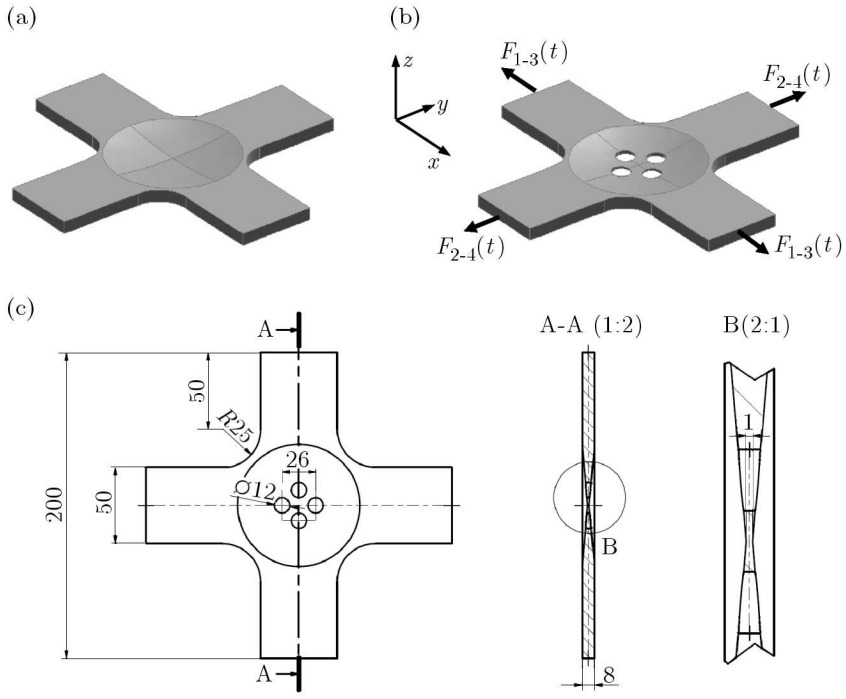

Fig. 1. Typical specimen for fatigue tests at the stand MZPK-100 (a) special specimen with holes and directions of force action (b) dimensions of the specimen (c)

The fatigue tests were performed at the stand MZPK-100 for tests of cruciform specimens under a biaxial plane stress state. While testing, the specimens were loaded by a random history of Gaussian distribution with a wide frequency band. An example of the time course is shown in Fig. 2. Random histories of forces $F_{1-3}(t)$ and $F_{2-4}(t)$ applied to the specimen arms were

obtained by filtration of noise of normal distribution, following that they were scaled to a suitable value of standard deviation for a given sample and arm pairs 1-3 and 2-4. Two series of tests were carried out. In series K01, the sense of force vector applied in one pair of arms was set inversely to the second pair $F_{1-3}(t) = -F_{2-4}(t)$, which led to the value of correlation coefficient $r_F = -1$. In series K02, the senses of applied forces were equal, $F_{1-3}(t) = F_{2-4}(t)$, and the correlation coefficient $r_F = 1$. During the fatigue tests, the specimen surface near the holes was observed using optical microscope – time and places of crack occurrences were registered. Figure 3 shows the initial place and path of the observed fatigue cracks in the specimens during tests K01 and K02. Table 2 contains time to cracks initiation obtained for particular cracks during the fatigue tests.

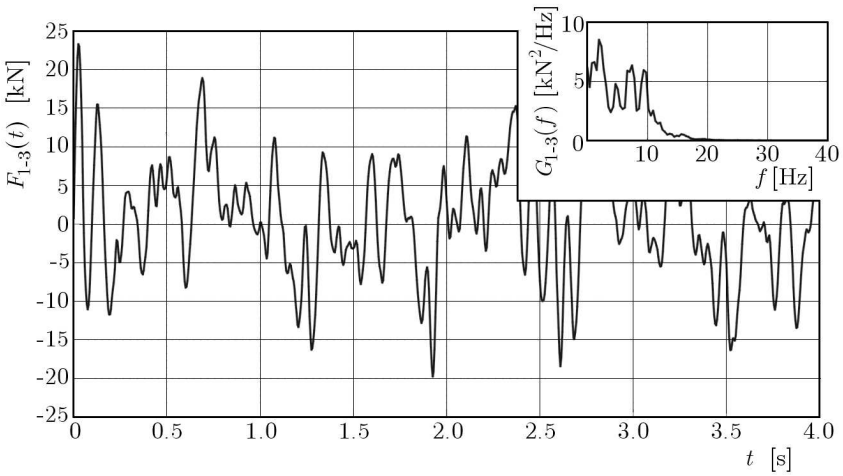

Fig. 2. A fragment of the random loading history registered by the force sensor during fatigue test

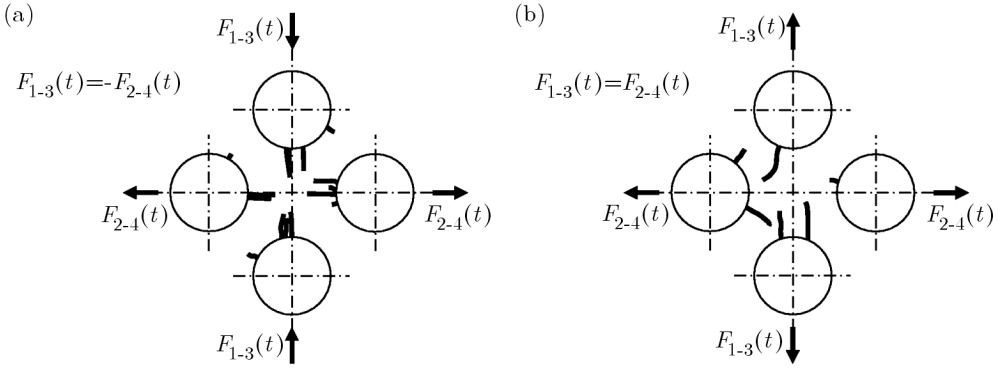

Fig. 3. Fatigue crack paths observed during the tests for all tested specimens, series K01 (a) and K02 (b)

3. Determination of fatigue crack initiation location

The main part of the algorithm, showing the location of fatigue crack initiation is presented in Fig. 4. There are three parts of the algorithm. The first part is responsible for the preparation for calculations, the next part – for fatigue calculations, and the last one concerns interpretation of calculation results. The algorithm uses the spectral method of fatigue life determination. This method is very efficient and suitable for the assumed type of loading. In the following subsections each part of the algorithm will be presented respectively to the object of analysis – the cruciform specimen with holes presented in Fig. 1.

Table 2. Time to the initiations of fatigue cracks presented in Fig. 3

Spec. No.	r_F (series of tests)	F_{1-3} [kN]	F_{2-4} [kN]	T_{cal} [s]	Crack No.	T_{exp} [s]
1	−1 (K01)	7.645	7.554	1911	1.1	1685
					1.2	1803
					1.3	2520
					1.4	2885
					1.5	4320*
					1.6	4320*
2	−1 (K01)	6.028	5.905	3930	2.1	2711
					2.2	2890
					2.3	3502
					2.4	4461
3	1 (K02)	12.74	12.57	60401	3.1	15210
					3.2	15942
					3.3	16060
					3.4	19650
					3.5	20767
4	1 (K02)	13.24	12.97	52517	4.1	15951
5	−1 (K01)	6.115	6.361	4038	5.1	2504
					5.2	2845
					5.3	3615
					5.4	3995
					5.5	3995
					5.6	4176

$*$ – crack detected after the test was stopped

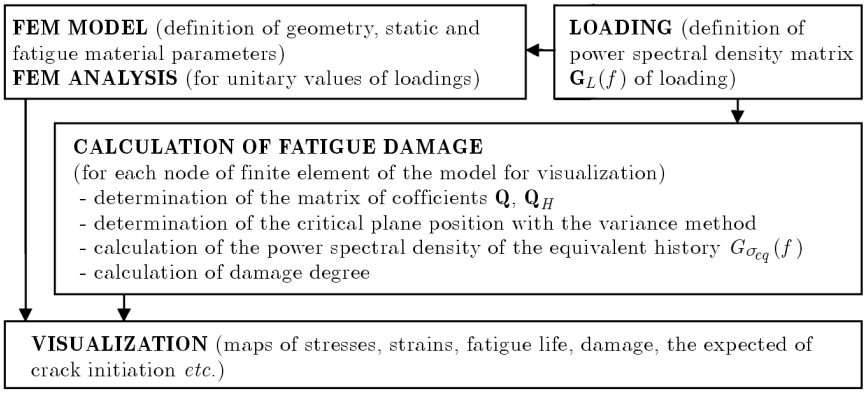

Fig. 4. Algorithm showing places of fatigue crack initiation

3.1. Preparations for fatigue calculations

At this stage, the specimens geometry is modelled and linear-elastic analyses of FEM are performed. Since the loading of the specimen was performed by two independent forces $F_{1-3}(t)$ and $F_{2-4}(t)$, two FEM models have been prepared and subjected to unitary loads. The symmetry of the sample was used to load only a quarter of the model. Free mesh option was used in the Comsol Multiphysics 3.5 FEM program for mesh generation with more detailed mesh near the holes, see Fig. 5. From the FEM results, the matrix of coefficients of transition $\mathbf{Q}$ between the unit value of global specimen loading $\mathbf{L}(t) = [F_{1-3}(t), F_{2-4}(t)]$ and the strain tensor components

in the specimen (Niesłony and Sonsino, 2006) can be defined. The strain tensor components are obtained by the following operation

$$\boldsymbol{\varepsilon}(t) = \mathbf{L}(t)\mathbf{Q} \tag{3.1}$$

where

$$\boldsymbol{\varepsilon}(t) = [\varepsilon_{xx}(t), \varepsilon_{yy}(t), \varepsilon_{zz}(t), \varepsilon_{xy}(t), \varepsilon_{xz}(t), \varepsilon_{yz}(t)] \tag{3.2}$$

The matrix of transition coefficients is defined as

$$\mathbf{Q} = \begin{bmatrix} Q_{xxF_{1-3}} & Q_{yyF_{1-3}} & Q_{zzF_{1-3}} & Q_{xyF_{1-3}} & Q_{xzF_{1-3}} & Q_{yzF_{1-3}} \\ Q_{xxF_{2-4}} & Q_{yyF_{2-4}} & Q_{zzF_{2-4}} & Q_{xyF_{2-4}} & Q_{xzF_{2-4}} & Q_{yzF_{2-4}} \end{bmatrix} \tag{3.3}$$

Assuming that the random loading process $\mathbf{L}(t)$ is ergodic and stationary, and its probability distribution can be described by a normal distribution, the power spectral density matrix $\mathbf{G}_L(f)$ with the 2×2 size was determined. Material constants describing static and fatigue properties of St52.3 structural steel were defined according to Table 1.

3.2. Calculation of damage degree

The subdomain of the specimen subjected to fatigue analysis is defined in the following step. In the considered case, it is the central part of the specimen including holes (see Fig. 5). Because of the symmetry, also in this case, only the quarter of the analysed area was modeled.

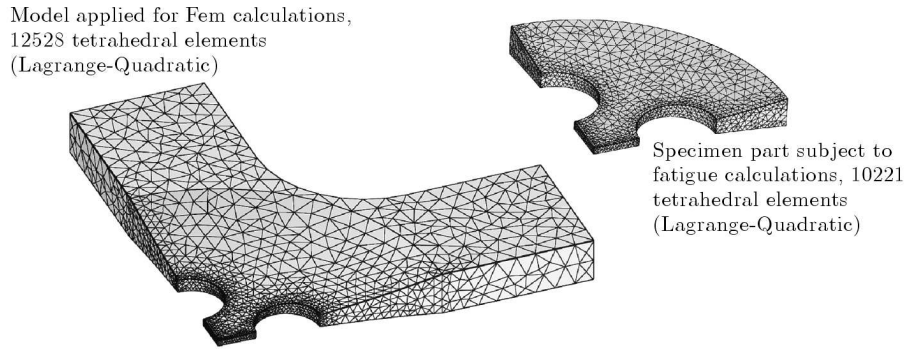

Fig. 5. A part of the specimen for determination of fatigue life maps

The FEM mesh was generated for the considered subdomain. It should be understood that the FEM mesh is not involved in FEM calculations, but is used only during the interpolation of results and visualization. This is one of the major advantages of the proposed algorithm, since it allows the fatigue analysis of selected parts of the structure regardless of the FEM analysis. Calculations can be performed repeatedly on the basis of interpolated to the mesh nodes values of coefficients $\mathbf{Q}$. The fatigue damage was determined for each node of the mesh; the calculation steps were the following:

STEP 1 – determination of the power spectral density matrix directly from the matrix of power spectral density of loading

$$\mathbf{G}_\sigma(f) = [\mathbf{Q}\mathbf{Q}_H]^\top \mathbf{G}_L(f)\mathbf{Q}\mathbf{Q}_H \tag{3.4}$$

where $\mathbf{Q}$ is the matrix of transition coefficients (3.33), $\mathbf{Q}_H$ is the matrix of coefficients of generalized Hooke's law written in the form

$$\mathbf{Q}_H = \frac{E}{(1+\nu)(1-2\nu)} \begin{bmatrix} 1-\nu & \nu & \nu & 0 & 0 & 0 \\ \nu & 1-\nu & \nu & 0 & 0 & 0 \\ \nu & \nu & 1-\nu & 0 & 0 & 0 \\ 0 & 0 & 0 & 1-2\nu & 0 & 0 \\ 0 & 0 & 0 & 0 & 1-2\nu & 0 \\ 0 & 0 & 0 & 0 & 0 & 1-2\nu \end{bmatrix} \tag{3.5}$$

STEP 2 – calculation of power spectral density of the equivalent stress history. During this stage of calculation, it is needed to choose the right multiaxial fatigue failure criterion. It is recommended that this criteria should be defined in the frequency domain, which allows the performance of efficient calculations, without the need to generate stress time courses on the basis of the PSD matrix of stress tensor components (3.4). A wider description of those sort of criteria can be found in many literature positions (Pitoiset and Preumont, 2000; Niesłony and Macha, 2007; Niesłony, 2010; Cristofori *et al.*, 2011; Susmel and Tovo, 2011). In order to perform calculations, it has been decided to use one of the linear multiaxial fatigue criteria, which allows one to determine the PSD function of the equivalent stress course according to the following formula

$$G_{\sigma_{eq}}(f) = \mathbf{a}\mathbf{G}_\sigma(f)\mathbf{a}^{\mathrm{T}} \tag{3.6}$$

where $\mathbf{a}$ is a vector of coefficients resulting from the multiaxial fatigue failure criterion under the assumed position of the critical plane (Łagoda and Ogonowski, 2005). The criterion of the maximum normal stress on the critical plane was applied (Grzelak *et al.*, 1991). According to this criterion, the equivalent stress is expressed as

$$\begin{aligned} \sigma_{eq}(t) = \sigma_\eta(t) &= l_\eta^2\sigma_{xx}(t) + m_\eta^2\sigma_{yy}(t) + n_\eta^2\sigma_{zz}(t) + 2l_\eta M_\eta\sigma_{xy}(t) \\ &+ 2l_\eta n_\eta\sigma_{xz}(t) + 2m_\eta n_\eta\sigma_{yz}(t) \end{aligned} \tag{3.7}$$

where l_η, m_η, n_η are directional cosines of the vector normal to the critical plane. Basing on Eq. (3.7), the vector of coefficients from the criterion $\mathbf{a}$ can be easily defined

$$\mathbf{a} = [l_\eta^2, m_\eta^2, n_\eta^2, 2l_\eta m_\eta, 2l_\eta n_\eta, 2m_\eta n_\eta] \tag{3.8}$$

The criterion is rather simple but it gives good results for stresses occurring at the edges of plane elements subjected to tension, because in such places there is a stress state similar to uniaxial tension-compression. The variance method was used for determination of the critical plane position (Łagoda *et al.*, 2005; Niesłony and Macha, 2007; Susmel, 2010). According to that method, the critical plane is the plane of the maximum variance of normal stress. The search of the critical plain position is usually performed through appointing the variance of normal stress for the closed set of planes $i \in (1, k)$ and selection of that of the greatest variance value, μ_{max}

$$\mu_{max} = \max_i(\mathbf{a}_i\boldsymbol{\mu}\mathbf{a}_i^{\mathrm{T}}) = \max_i\left(\mathbf{a}_i\int_0^\infty \mathbf{G}_\sigma(f)\,df\mathbf{a}_i^{\mathrm{T}}\right) \tag{3.9}$$

where μ_{max} is the maximum variance for the considered set of planes, $\mathbf{a}_i$ – vector of criterion coefficients for the i-th plane. The set of planes should be suitably wide and it should include all the possible positions of the critical plane.

STEP 3 – calculation of fatigue life T_{cal}. Because of the wide loading frequency band, the Dirlik proposal (Dirlik, 1985; Niesłony, 2010) was chosen for description of the probability distribution of loading cycles stress ranges

$$p(\Delta\sigma) = \frac{1}{2\sqrt{\xi_0}}\Big(\frac{K_1}{K_4}\mathrm{e}^{\frac{-Z}{K_4}} + \frac{K_2 Z}{R^2}\mathrm{e}^{\frac{-Z^2}{2R^2}} + K_3 Z\mathrm{e}^{\frac{-Z^2}{2}}\Big) \tag{3.10}$$

and

$$Z = \frac{\Delta\sigma}{2\sqrt{\xi_0}} \qquad K_1 = \frac{2(x_m - I^2)}{1 + I^2} \qquad K_2 = \frac{1 - I - K_1 + K_1^2}{1 - R}$$

$$K_3 = 1 - K_1 - K_2 \qquad K_4 = \frac{5(I - K_3 + K_2 R)}{4K_1} \qquad R = \frac{I - x_m - K_1^2}{1 - I - K_1 - K_1^2}$$

$$x_m = \frac{\xi_1}{\xi_0}\sqrt{\frac{\xi_2}{\xi_4}} \qquad I = \frac{\xi_2}{\sqrt{\xi_0 \xi_4}} \qquad \xi_k = \int_0^\infty G_{\sigma_{eq}}(f) f^k \, df$$

The model proposed by Dirlik is often applied and gives good results in the considered conditions. Moreover, using the model, Probability Density Function (PDF) of stress ranges can be estimated similarly to those obtained using the rainflow cycle counting method. This allows one to undergo transformation of the obtained PDF according to the Neuber method

$$p(\Delta\sigma_{tr}) = g(p(\Delta\sigma), E, n', K') \tag{3.11}$$

where $g(\cdot,\cdot)$ is the transformation function according to the Neuber rule. The procedure allows determination of approximate values of the elastic-plastic stresses under cyclic loading. Next, the fatigue damage accumulation was performed with the use of the linear Palmgren-Miner hypothesis for the whole stress range

$$T_{cal} = \left(M^+ \int_0^\infty \frac{p(\Delta\sigma_{tr})}{N(\Delta\sigma_{tr})} \, d\Delta\sigma_{tr} \right)^{-1} \tag{3.12}$$

where

$$M^+ = \sqrt{\frac{\xi_4}{\xi_2}} \qquad N(\Delta\sigma_{tr}) = \sigma_{af}^m N_0 \Big(\frac{\Delta\sigma_{tr}}{2} \Big)^{-m}$$

It should be noted that only a few materials can be correctly described with this hypothesis (Mroziński, 2011; Szala, 1998). One of them is the St52.3 steel. Other damage summation hypotheses are presented and well described for example in (Fatemi and Yang, 1998; Halford, 1997; Niesłony and Macha, 2007; Read and Shenoi, 1995). The limitations of linear damage accumulation hypotheses are well known to the authors, but it seems that the advantages of this method which is mainly: extremely easines of using and almost all alternative developed methods require at least one or more constants that must be experimentally determined (Manson and Halford, 2006), are relevant to the subject of this paper.

3.3. Visualization and analysis of the results

The fatigue damage map was made for the quarter of the central part of the specimen (Fig. 5b) including the area of fatigue crack occurrence for both test series. Figure 6 presents the obtained fatigue damage map using the value of damage logarithm $\log(1/T_{cal})$. All fatigue cracks from the specimen presented in Fig. 3 were superimposed on the resulting fatigue map of the quarter of the FEM modelled sample in order to directly compare the calculations with experimental results. The dark areas are characterized by lower fatigue life, and the fatigue crack initiation can be expected in those places. Comparing the obtained fatigue damage contours with the cracks, high correlation between the areas of maximum damage degree and the areas of real fatigue cracks can be noticed. In the case of test series K01, three such places were found for each hole, and two such places were found in test series K02 (see Fig. 6). From the calculation

results presented in Table 2 it appears that in the case of loading realized under $r_F = -1$, series K01, the calculated fatigue lifes are a little underrated as compared to the test results. The calculated fatigue lifes for $r_F = 1$, series K02, are greatly overestimated. It is probably caused by the occurrence of local plastic strains at the holes edge. Thus, another method of correction of the stress ranges than the Neuber rule, while fatigue life assessment based on the stress obtaining from linear-elastic FEM analysis should be considered.

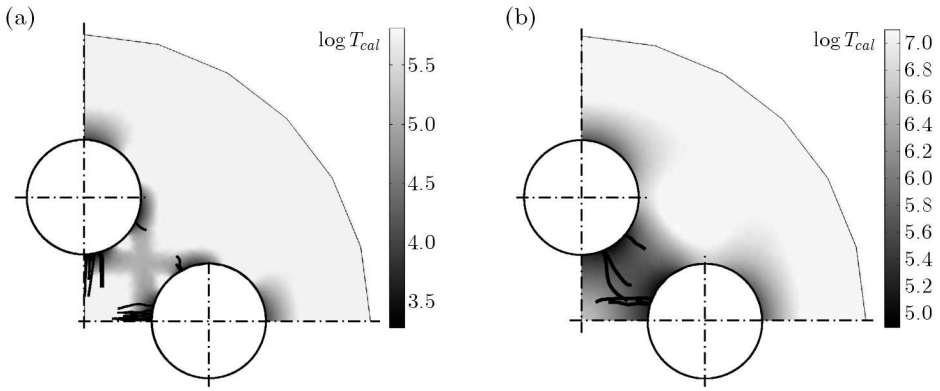

Fig. 6. Fatigue life map for the central part of the specimen for two test series: K01 (a) and K02 (b)

4. Conclusions

Cruciform specimens with holes were subjected to biaxial asynchronous (K01) and synchronous (K02) tension-compression. From analysis of the test results it appears that the obtained fatigue life maps (Fig. 6) allow one to predict the areas liable to crack initiation. These areas match (Fig. 3) with the areas of fatigue cracks initiation determined during the tests. The calculated fatigue lifes correlate with those obtained from the experiments.

Fatigue calculations were performed independently of linear-elastic analyses used for determination of the transition coefficients $\mathbf{Q}$. Thus, they could be realized many times for different loading conditions as post-processing routine. It strongly influences the rate of calculations because in the considered situation linear-elastic FEM analyses do not need to be repeated. Moreover, application of only a part of geometry for fatigue calculations allows making an efficient analysis only in one place, where the fatigue crack initiation is expected. In extreme cases, it may be at only one point (mesh node), but then the fatigue damage maps cannot be drawn. This fact is important in the fatigue analysis of so-called big FEM models (more than 1000 000 degrees of freedom), for which fatigue life calculations would be time-consuming. Selection of subdomains, where the fatigue life assessment is performed, is a simple solution allowing fatigue calculations also for big FEM models.

The proposed method should be implemented in FEM software and used by engineers for quick identification of the points of fatigue crack initiation. However, it should be developed for including the possibility of determination of the crack initiation direction, what is important for simulation of the crack propagation, and the accuracy of determination of time to crack initiation should be improved.

Acknowledgement

This paper is realized within the framework of research project No. 2011/01/B/ST8/06850 funded by National Science Centre in Poland.

References

1. Cristofori A., Benasciutti D., Tovo R., 2011, A stress invariant based spectral method to estimate fatigue life under multiaxial random loading, *International Journal of Fatigue*, **33**, 887-899
2. Dirlik T., 1985, Application of computers in fatigue analysis, Ph.D. Thesis, University of Warwick
3. Fatemi A., Yang L., 1998, Cumulative fatigue damage and life prediction theories: a survey of the state of the art for homogeneous materials, *International Journal of Fatigue*, **20**, 1, 9-34
4. Grzelak J., Łagoda T., Macha E., 1991, Spectral Analysis of the criteria for multiaxial random fatigue, *Materialwissenschaft und Werkstofftechnik*, **22**, 85-98
5. Halford G.R., 1997, Cumulative fatigue damage modelingcrack nucleation and early growth, *International Journal of Fatigue*, **19**, 253-260
6. Łagoda T., Macha E., Będkowski W., 1999, A critical plane approach based on energy concepts: application to biaxial random tension-compression high-cycle fatigue regime, *International Journal of Fatigue*, **21**, 431-443
7. Łagoda T., Macha E., Niesłony A., 2005, Fatigue life calculation by means of the cycle counting and spectral methods under multiaxial random loading, *Fatigue and Fracture of Engineering Materials and Structures*, **28**, 409-420
8. Łagoda T., Ogonowski P., 2005, Criteria of multiaxial random fatigue based on stress, strain and energy parameters of damage in the critical plane, *Materialwissenschaft und Werkstofftechnik*, **36**, 429-437
9. Macha E., Niesłony A., 2012, Critical plane fatigue life models of materials and structures under multiaxial stationary random loading: The state-of-the-art in Opole Research Centre CESTI and directions of future activities, *International Journal of Fatigue*, **39**, 95-102
10. Manson S.S., 1965, Fatigue: A complex subjectsome simple approximations, *Experimental Mechanics*, **5**, 193-226
11. Manson S.S., Halford G.R., 2006, *Fatigue and Durability of Structural Materials*, ASM International Ohio
12. Mroziński S., 2011, The influence of loading program on the course of fatigue damage cumulation, *Journal of Theoretical and Applied Mechanics*, **49**, 1, 83-85
13. Niesłony A., 2009, Determination of fragments of multiaxial service loading strongly influencing the fatigue of machine components, *Mechanical Systems and Signal Processing*, **23**, 2712-2721
14. Niesłony A., 2010, Comparison of some selected multiaxial fatigue failure criteria dedicated for spectral method, *Journal of Theoretical and Applied Mechanics*, **48**, 233-254
15. Niesłony A., Macha E., 2007, *Spectral Method in Multiaxial Random Fatigue*, Lecture Notes in Applied and Computational Mechanics, Springer Berlin, Heidelberg
16. Niesłony A., Sonsino C.M., 2006, Calculating the fatigue crack initiation in machine parts under random multiaxial loading, [In:] *COMSOL Multiphysics Konferenz 2006 – Neue Wege Der Multiphysik Simulation*, 106-111
17. Pitoiset X., Preumont A., 2000, Spectral methods for multiaxial random fatigue analysis of metallic structures, *International Journal of Fatigue*, **22**, 541-550
18. Read P.J.C.L., Shenoi R.A., 1995, A review of fatigue damage modelling in the context of marine FRP laminates, *Marine Structures*, **8**, 257-278
19. Schijve J., 2009, *Fatigue of Structures and Materials*, Springer Berlin, Heidelberg
20. Shamsaei N., Fatemi A., Socie D.F., 2011, Multiaxial fatigue evaluation using discriminating strain paths, *International Journal of Fatigue*, **33**, 597-609
21. Stephens R.I., Fuchs H.O., 2001, *Metal Fatigue in Engineering*, Wiley-IEEE

22. Susmel L., 2010, A simple and efficient numerical algorithm to determine the orientation of the critical plane in multiaxial fatigue problems, *International Journal of Fatigue*, **32**, 1875-1883

23. Susmel L., Tovo R., 2011, Estimating fatigue damage under variable amplitude multiaxial fatigue loading, *Fatigue and Fracture of Engineering Materials and Structures*, **34**, 1053-1077

24. Szala J., 1998, *Hipotezy sumowania uszkodzeń zmęczeniowych*, Wydawnictwa Uczelniane ATR w Bydgoszczy, 175 pp.

25. Zhang S., Sakane M., 2007. Multiaxial creep-fatigue life prediction for cruciform specimen, *International Journal of Fatigue*, **29**, 2191-2199

Zastosowanie metody spektralnej w wyznaczaniu trwałości zmęczeniowej – określanie inicjacji pęknięć

Streszczenie

Celem niniejszej pracy jest przedstawienie prostego podejścia w wyznaczaniu tych miejsc w elementach maszyn, gdzie nastąpi inicjacja pęknięć. Niniejsza metoda wykorzystuje metodę elementów skończonych (MES) i krzywą cyklicznego odkształcenia w celu obliczenia stanu naprężenia w próbkach. Wieloosiowe kryterium zmęczenia oparte na założeniach płaszczyzny krytycznej zostało zastosowane w celu redukcji przestrzennego losowego stanu naprężenia na ekwiwalentny jednoosiowy. Położenie płaszczyzny krytycznej zostało zdefiniowane przy pomocy metody wariancji, natomiast trwałość zmęczeniowa została wyznaczona zgodnie z założeniami liniowej hipotezy sumowania uszkodzeń. Weryfikacja eksperymentalna zaproponowanej metody została przeprowadzona na podstawie wyników badań zmęczeniowych stali konstrukcyjnej St52.3 poddanej dwuosiowym losowemu obciążeniu rozciąganiem-ściskaniem. W niniejszych badaniach zostały zastosowane próbki krzyżowe z czterema otworami. W trakcie badań były rejestrowane miejsca oraz czas inicjacji pęknięcia. Wykazano, że proponowana metoda wyznaczania miejsc inicjacji pęknięć dała wyniki pokrywające się z otrzymanymi w trakcie eksperymentu. Proponowana metoda może zostać zastosowana przez inżynierów w celu identyfikacji miejsc oraz czasu, w którym nastąpi inicjacja pęknięć zmęczeniowych.

Manuscript received February 3, 2012; accepted for print March 6, 2012